Electronic Supplementary Information

A Room-Temperature Aqueous Phosphorescent Probe for Gd^{3+}

Jiazhuo Li, Ying Wang, Xiaoming Jiang,* Peng Wu*

Analytical & Testing Center, State Key Laboratory of Hydraulics and Mountain River Engineering, Sichuan University, Chengdu 610064, China

*Corresponding author:

jiangxm@scu.edu.cn (X. Jiang)

wupeng@scu.edu.cn (P. Wu)

Table of Contents

Section S1. Experimental Section

S1.1 Materials

(1) Metal ions: $GdCl_3·6H_2O$, $LaCl_3·6H_2O$, $CeCl_3·6H_2O$, $PrCl_3·6H_2O$, $NdCl_3·6H_2O$, $SmCl_3·6H_2O$, $EuCl_3·6H_2O$, $TbCl_3·6H_2O$, $DyCl_3·6H_2O$, $HoCl_3·6H_2O$, $ErCl_3·6H_2O$, $TmCl_3·6H_2O$, $YbCl_3·6H_2O$, $LuCl_3·6H_2O$, $ScCl_3·6H_2O$, $YCl_3·6H_2O$, KCl, NaCl, $MgCl_2$, $FeCl_3·6H2O$, $MnCl_2$, VCl_3, $CoCl_2·6H_2O$, $CdCl_2$, $CuCl_2$, $ZnCl_2$, $MoCl_5$, $SeCl_4$, $NiCl_2$;

(2) Nucleotides: adenosine 5’-monophosphate disodium salt (AMP), guanine 5’-monophosphate disodium salt (GMP), thymine 5’-monophosphate disodium salt (TMP), cytidine 5’-monophosphate disodium salt (CMP);

(3) Dyes: fluorescein (FL), 2',4',5',7'-tetrabromofluorescein (EY), 2',4',5',7'-tetrabromo-3,4,5,6 of HEPES in water and adjusting to pH 6.2、6.4、 6.6、 6.8、 7.0、 7.2、 7.4、 7.6、 7.8、 8.0、8.2 with concentrated NaOH. Ultra-pure water was purified with a Direct--tetrachlorofluorescein (PB);

(4) Buffer: N-2-Hydroxyethyl piperazine-N'-2-ethanesulfonic acid (HEPES). HEPES buffer (50 mM, pH 7.4) was prepared by dissolving appropriate amounts Q system (Millipore Co.).

All above materials were purchased from Aladdin Reagent Database Inc. (Shanghai, China).

S1.2 Apparatus

All the instrumental information used for characterizations were given in Table S1.

Table S1. The instrumental information used in this work.

Characterization items	Type	Manufacturer
UV/Vis absorption spectra	Lambda-365 spectormeter	Perkin Elmer, USA
Fluorescence and phosphorescence spectra	FluoroMax-4P spectrofluorometer	Horiba Scientific, USA
Phosphorescence lifetime & QY	Fluolog-3 spectrofluorometer with an integration sphere (IS80, Labsphere) Fluorescence lifetime excitation: DeltaDiode (495 nm)	Horiba Jobin Yvon, USA
Transient absorption spectra	EOS	Ultrafast Systems, USA
$^1O_2$ phosphorescence emission	Fluolog-3 spectrofluorometer NIR Detector (H10330, Hamamatsu)	Horiba Jobin Yvon,USA
Dynamic light scattering	Zetasizer Nano ZS	Malvern, England
Scanning electron microscope	JSM-7500F	Japan electron optics laboratory co., ltd, Japan
Transmission electron microscope	Tecnai G2 F20 S-TWIN	FEI, USA
Fourier Transform infrared spectra	INVENIO®R	Bruker, Germany
Confocal Laser Microscope	N-SIM/A1R MP+	Nikon, Japan

S1.3 General experimental details

Synthesis of FL@Gd^{3+}/AMP CPNs.

The synthesis method used in this work was based on previous publication.[1] In practical terms, l mL of 10 mM aqueous solution of $GdCl_3 \cdot 6H_2O$ was added to 1 mL mixed solution of AMP (5 mM) and fluorescein (75 μM) which were dissolved in HEPES buffer (50 mM, pH 7.4), orange-yellow precipitates were formed immediately. After stirring for 3 h at room temperature, these precipitates were collected by centrifugation at 1000 rpm for 5 min and washed with ultra-pure water several times. Finally, the resulting precipitates were re-dispersed in HEPES buffer (50 mM, pH 7.4) and stored at room temperature for use.

Characterization of the FL@Gd^{3+}/AMP CPNs.

The suspensions of CPNs were ultrasonicated for 10 min before CLSM measurement (Fig. S1D). Then the well-dispersed CPNs were subjected to 50-fold dilution with HEPES buffer solution (50 mM, pH 7.4) for DLS (Fig. S6B), SEM (Fig. S7A) and TEM (Fig. S7B) measurements. After freeze drying the suspensions in vacuum (FD-1A-50, Bolcool), the obtained CPNs were collected for XRD and FTIR (Fig. S4) analysis. The UV-vis absorption, fluorescence emission and phosphorescence emission spectra were recorded based on the 5-fold diluted suspensions of CPNs.

Evaluation of the stability of the FL@Gd^{3+}/AMP CPNs.

The stability of FL@Gd^{3+}/AMP CPNs in HEPES buffer solution was tested by recording the RTP intensities of CPNs stored at room temperature for 1-14 days. The RTP intensity was closely related to the encapsulation efficiency (EE%) of coordination networks for FL. EE% can be calculated using the equation bellow[2].

$$EE\% = \frac{Wi - Ws}{Wi} \times 100\%$$

Ws is the amount of unbound dyes, and Wi is the total amount of dyes added initially during preparation. Ws can be determined by measuring the UV-vis absorbance of the supernatant after centrifugation of the suspensions of CPNs (Fig. S5). Herein, the EE% of CPNs was calculated to be larger than 95% with a colorless supernatant (the UV-vis absorbance is measured to be 0.0685), suggesting high encapsulation efficiency of AMP/Gd^{3+} networks for fluorescein. As shown in Figure S10, there was no significant change in the UV-vis absorbance of the supernatants recorded during 1-14 days, as well as the RTP intensities of CPNs, meaning a negligible leakage of guest FL molecules from the robust coordination networks.

Measurement of the 1275 nm phosphorescence emission of $^1O_2$.

For better collection of the characterized singlet oxygen phosphorescence emission (1275 nm), CH_3CN and D_2O mixed solvent (V_{CH3CN}:V_{D2O} = 15:1) was used to dissolve the vacuum-dried FL@Gd^{3+}/AMP CPNs and corresponding fluorescein molecules (10 mM), the final volume was 2 mL. Then the $^1O_2$ 1275 phosphorescence emission was measured on a Fluolog-3 spectrofluorometer equipped with a near-infrared (NIR) detector (H10330, Hamamatsu).

Measurement of the absolute luminescence quantum yield.

The luminescence quantum yields of FL before and after encapsulated into the AMP/Gd^{3+} networks were measured and compared by Fluolog-3 spectrofluorometer with an integration sphere (IS80, Labsphere) in this work. Herein, the suspension of AMP/Gd^{3+} CPNs was used as a blank control to extract the scattering interference of nanoparticles. The 5-fold diluted suspensions of FL@Gd^{3+}/AMP CPNs and the pure fluorescein solution (7.5 μM) were prepared for the measurement. The peak areas of fluorescence emission, RTP emission and integration absorption are integrated by origin 2016. After encapsulated into the AMP/Gd^{3+} networks, the fluorescence quantum yield of fluorescein reduced from 73.1% to 16.2%. However, the absolute RTP quantum yield of FL@Gd^{3+}/AMP CPNs was determined to be as high as 3.81%, while no RTP can be directly collected in FL solution.

Optimization of the experimental conditions for the RTP probe.

To achieve the optimal analytical performances of the developed RTP probe, different experimental parameters, including pH of the test solution, the kind of nucleotide ligand, the concentration of AMP and FL. Figure S12A showed the largest RTP response was obtained when AMP was choose as the nucleotide ligand, and 0.2 μM were the optimum concentration for probe fabrication (Fig. S12C). And the optimum concentration of guest FL molecules was 15 μM (Fig. S12D). Figure S12B demonstrated that the RTP probe can response for Gd^{3+} ions in neutral pH condition, so we launched the following detection procedure in HEPES buffer with pH 7.3.

Owning to an extremely fast formation of CPNs, the RTP intensity can reach the maximum value within 10 s after 1 mM Gd^{3+} was added. For sufficient reaction of the mixture, we mixed and allowed the solution to stand for another 2 minutes before recorded the spectra.

Heavy atom effect.

To explore the heavy atom effect induced by Gd, a series of FL solutions were prepared by "spiking" them with standard solution of Gd^{3+} ions. The phosphorescence lifetime of FL is difficult to be collected with the typical multichannel scanning technique due to the weak phosphorescence and strong interference from the fluorescence signal. Therefore, we employed the flash lamp for rough evaluation of the phosphorescence decay[3].

Detection selectivity of the RTP probe.

For the experiment of selectivity, stock solutions of $GdCl_3·6H_2O$, $LaCl_3·6H_2O$, $CeCl_3·6H_2O$, $PrCl_3·6H_2O$, $NdCl_3·6H_2O$, $SmCl_3·6H_2O$, $EuCl_3·6H_2O$, $TbCl_3·6H_2O$, $DyCl_3·6H_2O$, $HoCl_3·6H_2O$, $ErCl_3·6H_2O$, $TmCl_3·6H_2O$, $YbCl_3·6H_2O$, $LuCl_3·6H_2O$, $ScCl_3·6H_2O$ and $YCl_3·6H_2O$ (10 mM) were prepared with H_2O as solvent. 400 μL of 1 mM stock solutions of these interference ions were added to the mixing solution of AMP (0.1 mM) and FL (0.03 mM) respectively, the final volume was 2 mL. After reacting for 2 min at room temperature, the phosphorescence intensities of these mixtures at 630 nm were measured at 490 nm excitation wavelength. To explore the

mechanism underlying the detection specificity for Gd^{3+} of the RTP probe, FL@Eu^{3+}/AMP, EY@Eu^{3+}/AMP, PB@Eu^{3+}/AMP CPNs were formed following the same steps as FL@Gd^{3+}/AMP CPNs. The CPNs were subjected to 5-fold dilution with HEPES buffer solution before recording the phosphorescence emission and excitation spectra. The corresponding concentration of Eu^{3+}, Eu^{3+}/AMP and Eu^{3+}/FL were prepared and measured in the same test condition as CPNs. Emission was measured using long-pass filters (> 409 nm).

S2. Characterization of FL@Gd^{3+}/AMP CPNs

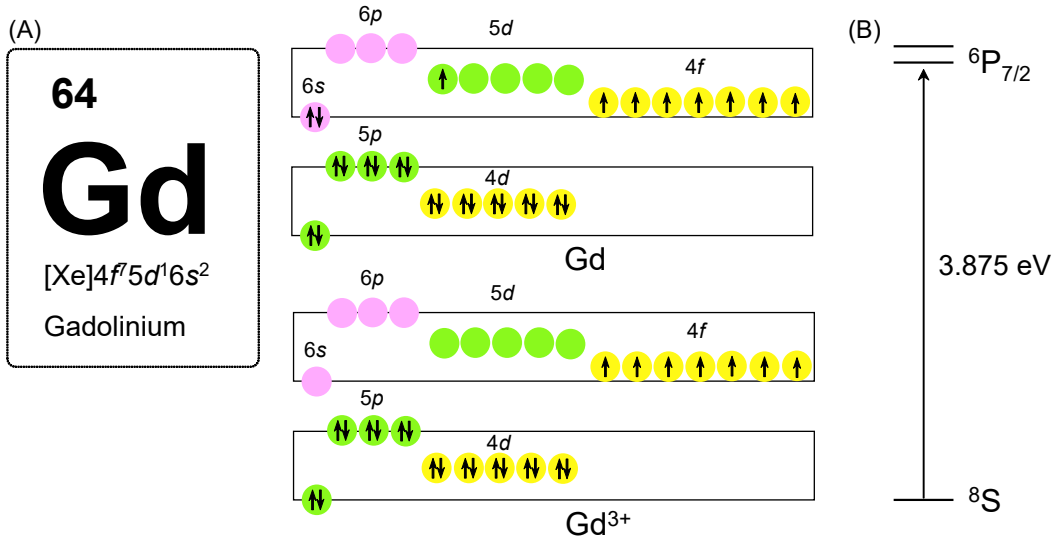

Figure S1. The electronic configuration of Gd and Gd^{3+}.

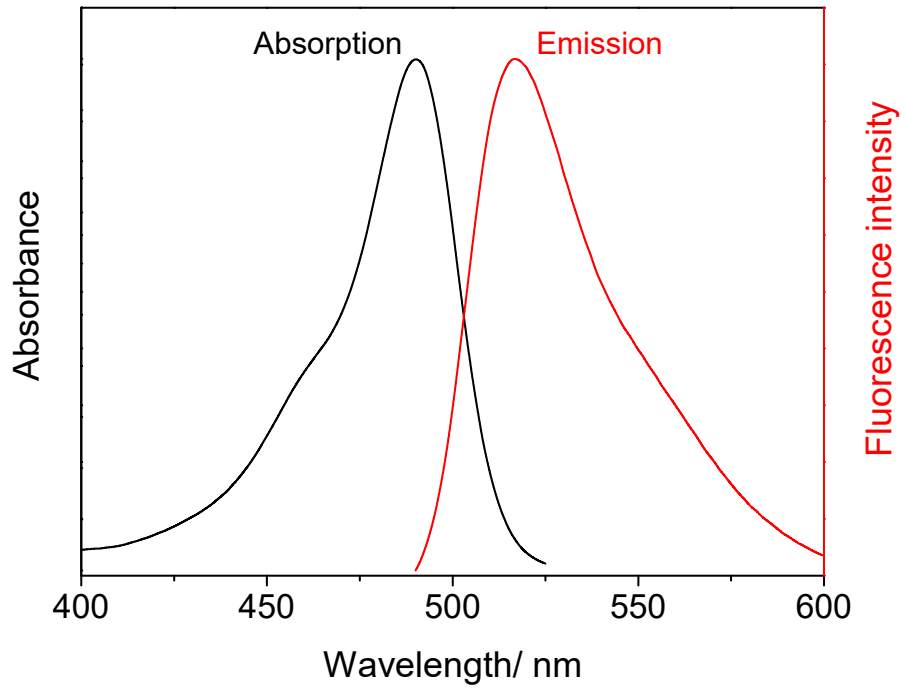

Figure S2. UV-vis absorption and fluorescence emission of fluorescein.

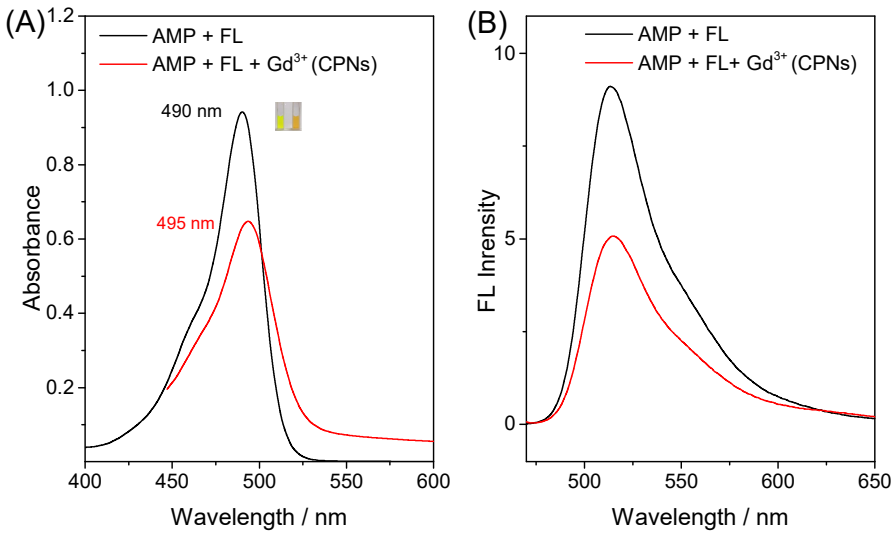

Figure S3. Characterizations of FL@Gd^{3+}/AMP CPNs: (A) UV−vis absorption spectra of fluorescein and CPNs; (B) fluorescence emission spectra of fluorescein and CPNs; (C) XRD of CPNs; and (D) DLS analysis of CPNs.

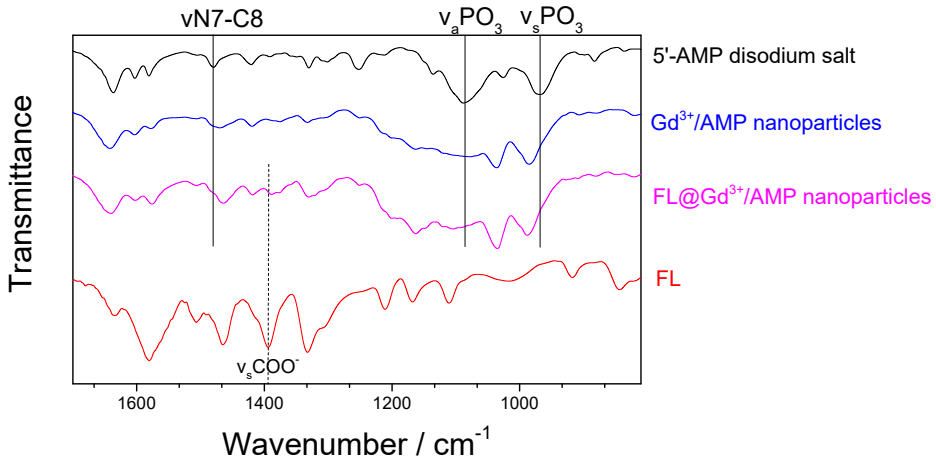

Figure S4. FTIR spectra of AMP, Gd^{3+}/ AMP, FL@ Gd^{3+}/ AMP CPNs and FL.

Fourier transform infrared spectroscopy (FT-IR) (Fig. S2) of AMP and AMP/Gd^{3+} showed changes in wavenumbers of phosphate (1090 cm^{-1} to 1099 cm^{-1} and 970 cm^{-1} to 985 cm^{-1}) and C-N stretching vibrations of adenine (1497 cm^{-1} to 1469 cm^{-1}), indicating that both phosphate and nucleobase moiety of AMP were involved in the coordination with Gd^{3+}. The FTIR spectrum of FL@Gd^{3+}/AMP is similar to that of AMP/Gd^{3+}, indicating encapsulation of fluorescein did not change the self-assembly behavior of AMP/Gd^{3+}. And the wavenumber changes of symmetrical stretching vibration of carboxylic anion (1394 cm^{-1} to 1388 cm^{-1}) indicated coordination of carboxylate groups to Gd^{3+} ions, which guaranteed the high (> 95%) for guest fluorescein molecules (Fig. S3).

Table S2. Changes in wavenumbers of stretching vibrations in figure S2.

	wavenumber (cm^{-1})		
	ν(N7-C8)	$\nu_a(PO_3)$	$\nu_s(PO_3)$
5'-AMP disodium salt	1479	1090	970
Gd^{3+}/AMP nanoparticles	1469	1099	985
FL@Gd^{3+}/AMP nanoparticles	1469	1099	985

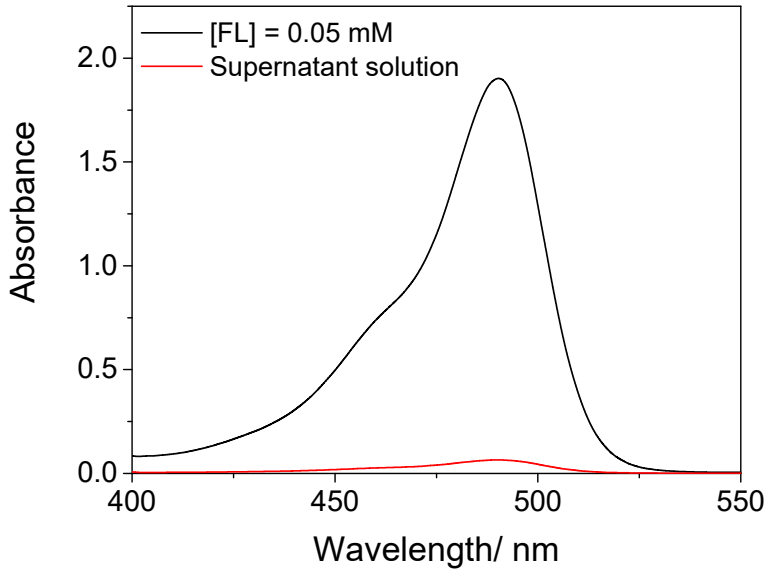

Figure S5. UV/vis absorption spectra of aqueous dye (black line, [dye] = 0.05 mM and aqueous supernatant obtained after centrifugation of aqueous FL@Gd^{3+}/AMP CPNs (red line, [AMP] = 2.5 mM, [Gd^{3+}] = 5 mM, [dye] = 0.05 mM). The ratio of dyes encapsulated in nanoparticles was determined from the absorption intensity of aqueous supernatant. Fluorescein molecules were nearly quantitatively bound to NPs (bound ratio: 96 %). Quartz cell with 1-cm path length was used.

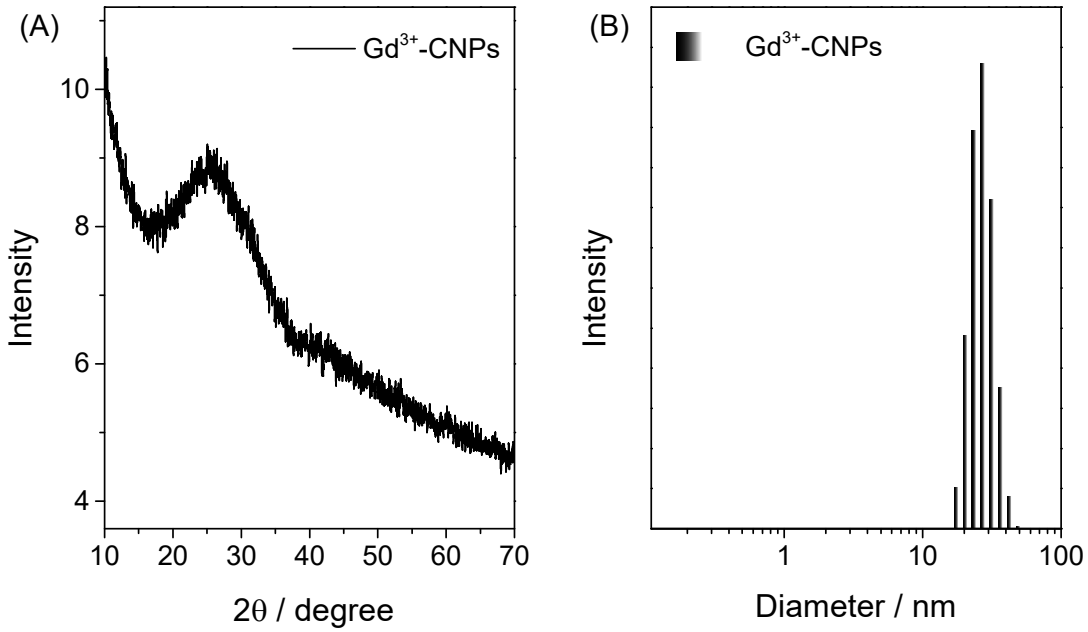

Figure S6. Characterizations of FL@Gd^{3+}/AMP CPNs. (A) XRD and (B) DLS analysis of CPNs.

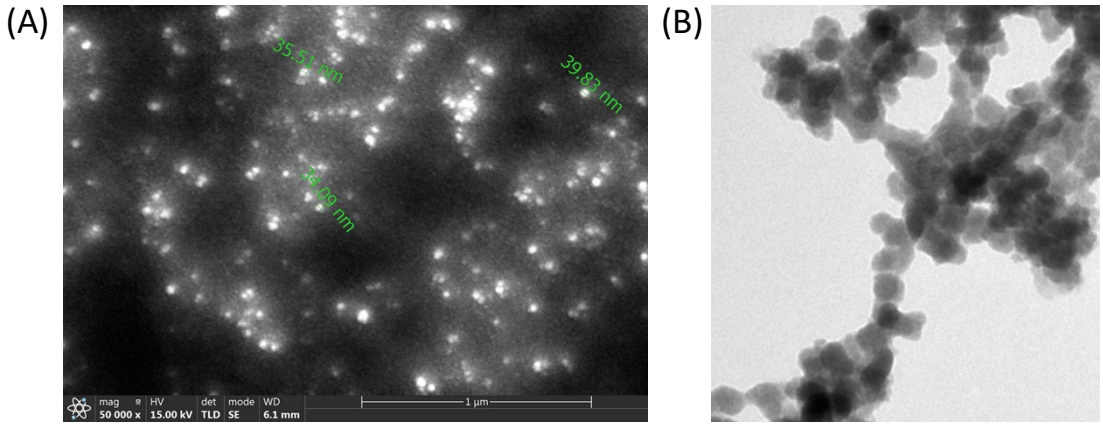

Figure S7. Characterizations of FL@Gd^{3+}/AMP CPNs. (A) SEM and (B) TEM micrograph of FL@Gd^{3+}/AMP CPNs collected on a conductive silicone after coated with Au.

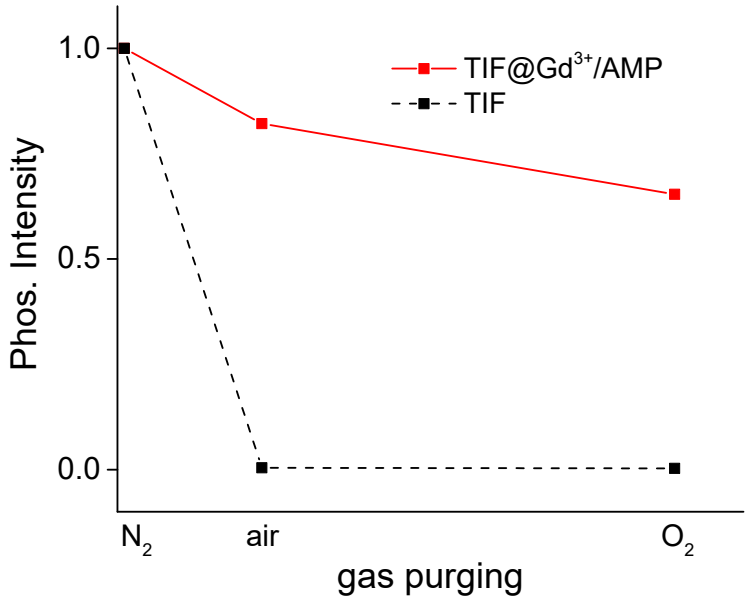

Figure S8. Oxygen-sensitive responses of RTP from TIF (tetraiodofluorescein) and TIF-included CPNs.

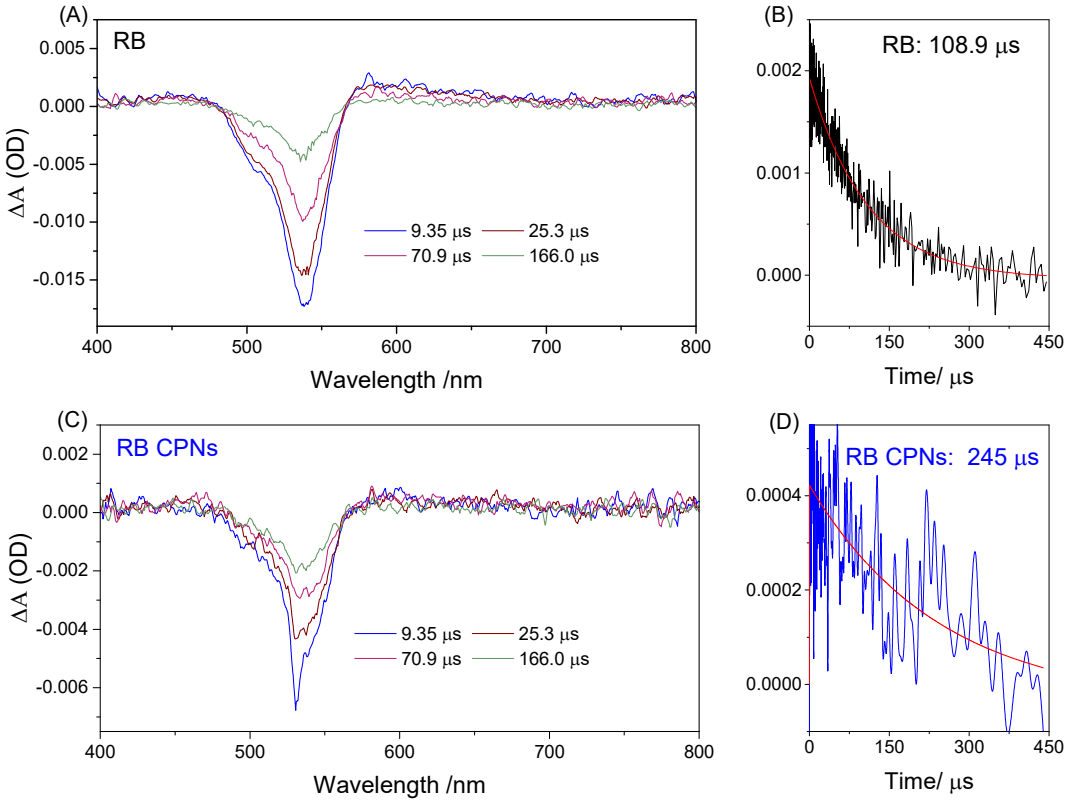

Figure S9. Transient absorption spectra of RB (A) and RB NPs (C) upon 532 nm laser excitation. The inset shows the time profile for ΔOD of RB (B) and RB NPs (D) recorded at 600 nm.

To facilitate the collection of nanosecond transient absorption spectra, fluorescein was replaced with rose Bengal (RB). On one hand, RB is a structural derivate of fluorescein. On the other hand, among the derivatives of fluorescein, only RB exhibited detectable signal before and after encapsulation.

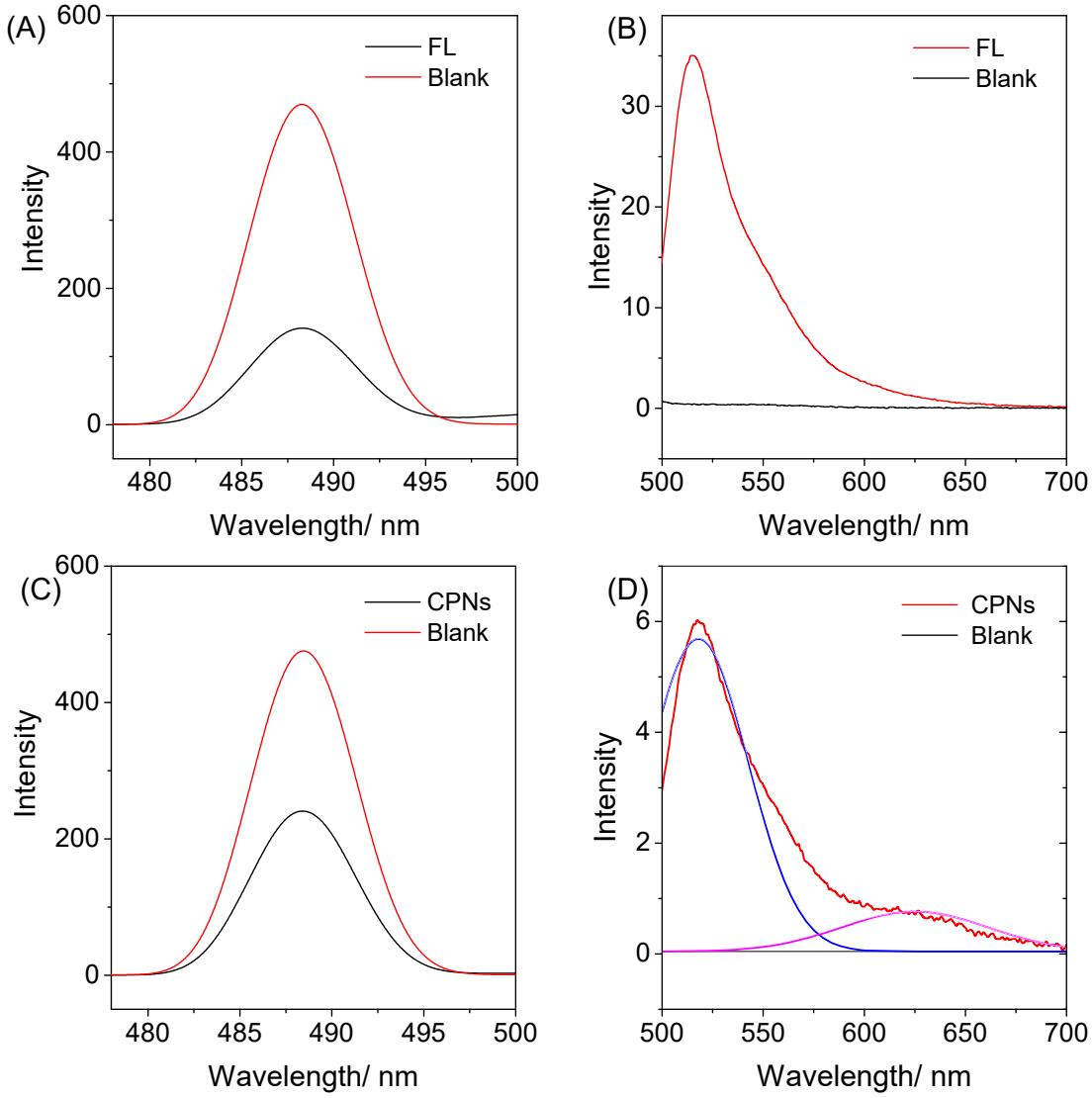

Figure S10. Luminescent quantum yields test. The absorbance (A) and the luminescence emission (B) spectra of FL in HEPES buffer solution. (λex = 490 nm, ΦFL = 73.1%). The absorbance (C) and the luminescence emission (D) spectra of FL@Gd3+/AMP CPNs dispersed in HEPES buffer solution. (λex = 490 nm, ΦFL = 16.2%, Φphos. =3.8%).

To confirm the potential confinement effect, radiative (k_r) and nonradiative (k_{nr}) transition constants were calculated through the following equations:[4]

$$\emptyset = \frac{k_r}{k_r + k_{nr}} \quad (1)$$

$$\tau = \frac{1}{k_r + k_{nr}} \quad (2)$$

$$k_{nr} = \frac{1 - \emptyset}{\tau} \quad (3)$$

Φ and τ are the quantum yield and lifetime of fluorescence or phosphorescence, respectively. Detailed measurements of $\Phi_{Fluo.}$, $\Phi_{Phos.}$, $\tau_{Fluo.}$, and $\tau_{Phos.}$ are given in the Supporting Information.

Table S3. Summary of the photophysical parameters of FL before and after being encapsulated into AMP/Gd^{3+} networks.

Parameters	Fluorescein (1)	CPNs (2)	(2) / (1)
$\Phi_{Fluo.}$ (%)	73.1	16.2	0.22
$\tau_{Fluo.}$ (ns)	4.1	2.0	0.49
k_r (Fluo.,10^8 s^{-1})	1.8	0.8	0.44
k_{nr} (Fluo.,10^8 s^{-1})	0.7	4.3	6.14
$\Phi_{Phos.}$ (%)	<0.001 [a]	3.8	~3800
$\tau_{Phos.}$ (ms)[b]	0.29	1.24	2.5
k_r (Phos, s^{-1})	0.034	30.6	890
k_{nr} (Phos, s^{-1})	3.45×10^3	0.78×10^3	0.22

a: for calculation, $\Phi_{Phos.}$ = 0.001%
b: collected with a FluorMax-4P spectrometer with flash lamp as excitation

Section S3. The optimization of detection conditions

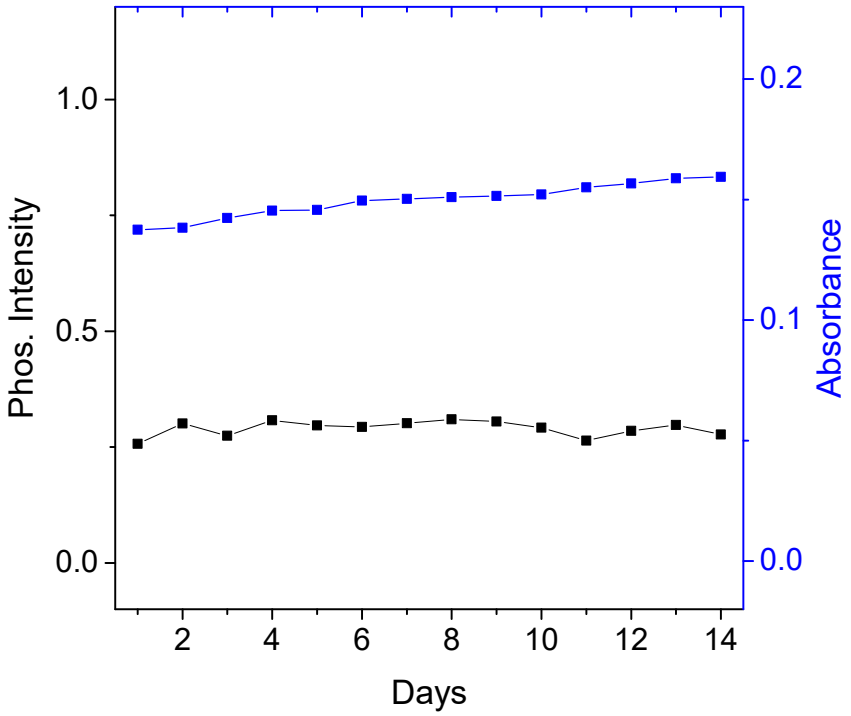

Figure S11. The UV-vis absorbance (at 490 nm) of supernatants and the RTP intensity (at 630 nm) of FL@Gd^{3+}/AMP CPNs measured during 14 days.

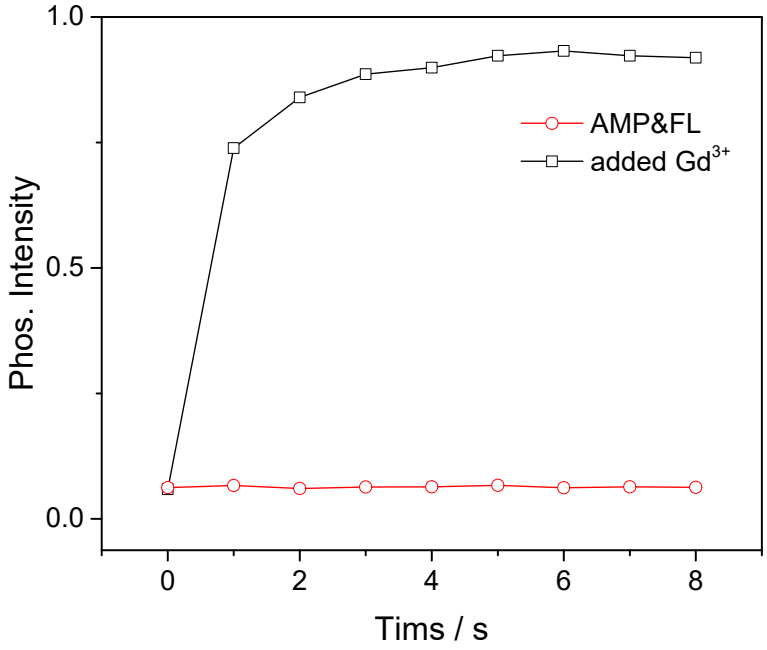

Figure S12. Effect of interaction time on RTP intensity of AMP&FL solution in the absence (red) and presence (black) of 1 mM Gd^{3+}. (λex = 490 nm; λem = 630 nm).

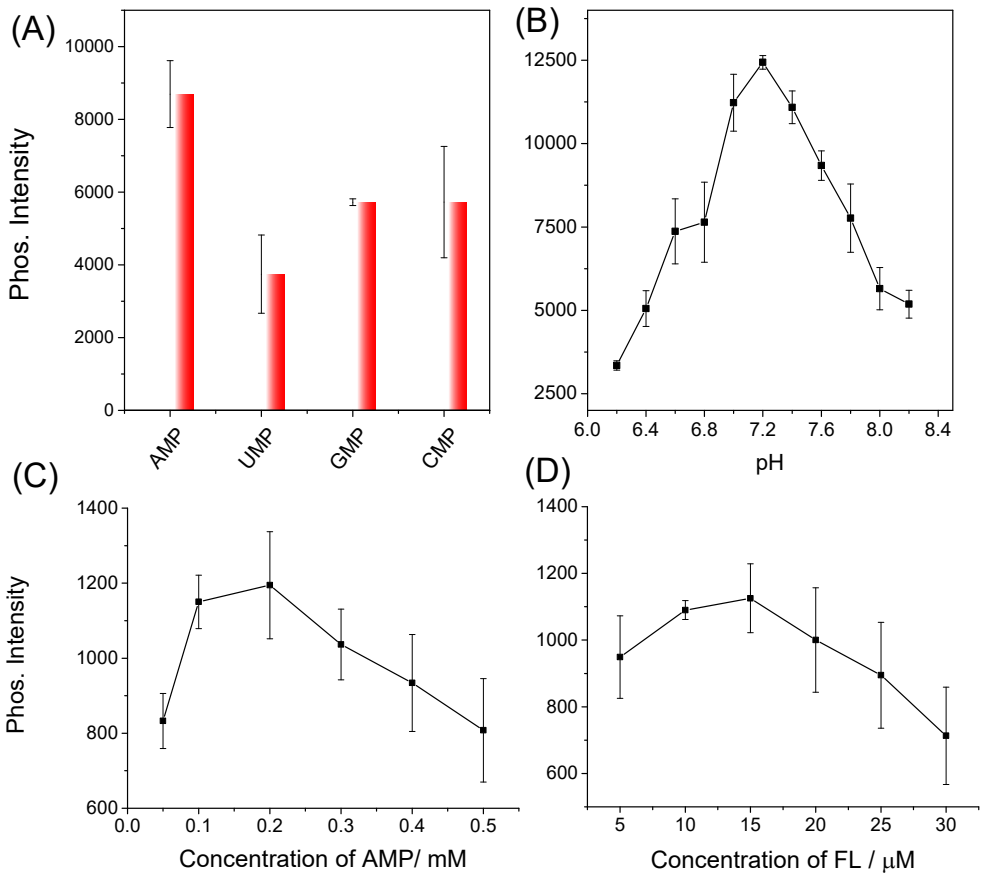

Figure S13. Effects of different experimental conditions on photocurrent: (A) the kind of nucleotide used as coordination ligand; (B) the pH of the test solution; the concentration of (C) AMP and (D) FL. All of the corresponding RTP signals were performed in 50 mM HEPES buffer (pH 7.4) containing 100 μM Gd^{3+} with 490 nm excitation light. Error bars: SD, n = 3.

Section S4. Mechanism of detection selectivity of the RTP probe

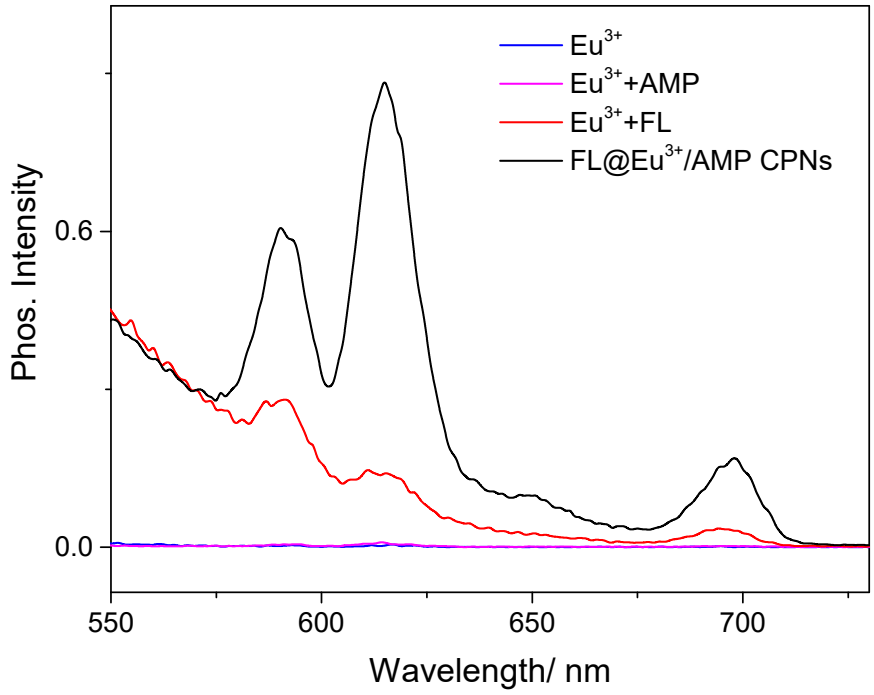

Figure S14. The phosphorescence emission spectra of Eu^{3+}, Eu^{3+}/AMP, Eu^{3+}/FL and FL@Eu^{3+}/AMP CPNs (λex = 490 nm).

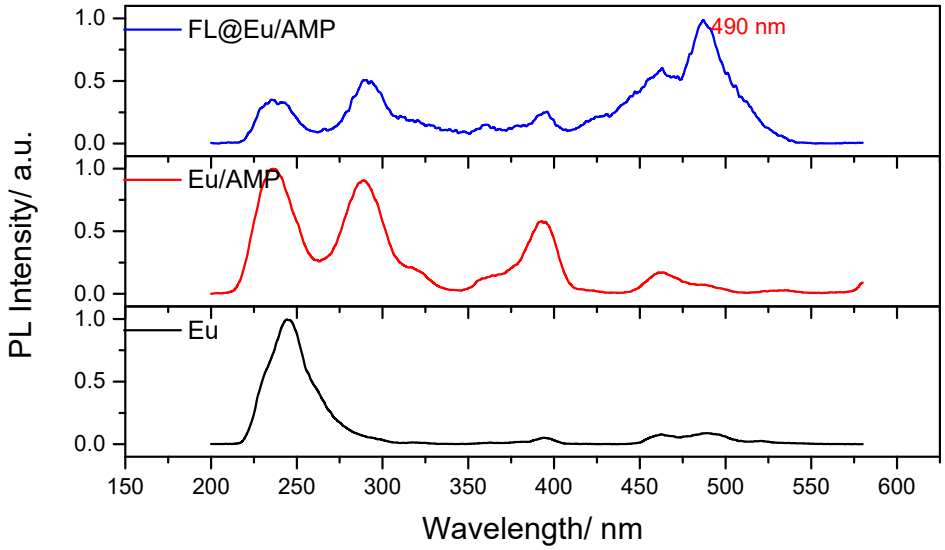

Figure S15. The phosphorescence excitation spectra of Eu^{3+}, Eu^{3+}/AMP, and FL@ Eu^{3+}/AMP and (λem = 694 nm).

References:

1. R. Nishiyabu, N. Hashimoto, T. Cho, K. Watanabe, T. Yasunaga, A. Endo, K. Kaneko, T. Niidome, M. Murata, C. Adachi, Y. Katayama, M. Hashizume and N. Kimizuka, *J. Am. Chem. Soc.*, 2009, **131**, 2151.

2. S. Daneshmand, S. Golmohammadzadeh, M. R. Jaafari, J. Movaffagh, M. Rezaee, A. Sahebkar and B. Malaekeh-Nikouei, *J. Cell. Biochem.*, 2018, **119**, 4251.

3. Y. Wang, H. Chen, C. Li and P. Wu, *Dyes Pigment.*, 2019, **170**, 107635.

4. (a) Y. Y. Wang, H. Hu, T. Y. Dong, H. Mansour, X. F. Zhang, F. Li and P. Wu, *CCS Chem.*, 2020, **2**, 2394; (b) Y. Y. Wang, R. H. Zhou, W. X. Liu, C. Liu and P. Wu, *Chin. Chem. Lett.*, 2020, **31**, 2950.

5. Y. Cui, Y. Yue, G. Qian and B. Chen, *Chem. Rev.*, 2012, **112**, 1126.